Interaction of Cardiac Troponin C with Ca^{2+} Sensitizer EMD 57033 and Cardiac Troponin I Inhibitory Peptide†

Monica X. Li,‡ Leo Spyracopoulos,‡ Norbert Beier,§ John A. Putkey,|| and Brian D. Sykes*,‡

MRC Group in Protein Structure and Function, Department of Biochemistry, University of Alberta, Edmonton, Alberta, Canada T6G 2H7, E. Merck, Department of Pharmaceutical Research, Frankfurter Strasse 250, 64271 Darmstadt, Germany, and Department of Biochemistry and Molecular Biology, University of Texas Medical School, Houston, Texas 77225

Received March 1, 2000; Revised Manuscript Received May 12, 2000

ABSTRACT: The binding of Ca^{2+} to cardiac troponin C (cTnC) triggers contraction in cardiac muscle. In diseased heart, the myocardium is often desensitized to Ca^{2+}, leading to weak cardiac contractility. Compounds that can sensitize cardiac muscle to Ca^{2+} would have potential therapeutic value in treating heart failure. The thiadiazinone derivative EMD 57033 is an identified 'Ca^{2+} sensitizer', and cTnC is a potential target of the drug. In this work, we used 2D {^{1}H, ^{15}N}-HSQC NMR spectroscopy to monitor the binding of EMD 57033 to cTnC in the Ca^{2+}-saturated state. By mapping the chemical shift changes to the structure of cTnC, EMD 57033 is found to bind to the C-domain of cTnC. To test whether EMD 57033 competes with cardiac TnI (cTnI) for cTnC and interferes with the inhibitory function, we examined the interaction of cTnC with an inhibitory cTnI peptide (residues 128−147, cIp) in the absence and presence of EMD 57033, respectively. cTnC was also titrated with EMD 57033 in the presence of cIp. The results show that although both the drug and cIp interact with the C-domain of cTnC, they do not displace each other, suggesting noncompetitive binding sites for the two targets. Detailed chemical shift mapping of the binding sites reveals that the regions encompassing helix G-loop IV-helix H are more affected by EMD 57033, while residues located on helix E-loop III-helix F and the linker between sites III and IV are more affected by cIp. In both cases, the binding stoichiometry is 1:1. The binding affinities for the drug are 8.0 ± 1.8 and 7.4 ± 4.8 μM in the absence and presence of cIp, respectively, while those for the peptide are 78.2 ± 10.3 and 99.2 ± 30.0 μM in the absence and presence of EMD 57033, respectively. These findings suggest that EMD 57033 may exert its positive inotropic effect by not directly enhancing Ca^{2+} binding to the Ca^{2+} regulatory site of cTnC, but by binding to the structural domain of cTnC, modulating the interaction between cTnC and other thin filament proteins, and increasing the apparent Ca^{2+} sensitivity of the contractile system.

Heart muscle contraction is regulated by contractile proteins. These include myosin, actin, tropomyosin, and troponin. Troponin is composed of three subunits: troponin C (TnC),[1] troponin I (TnI), and troponin T (TnT). In the relaxed state, the troponin complex holds tropomyosin in a conformational state that blocks the interaction between myosin and actin. When Ca^{2+} binds to troponin C, the troponin−tropomyosin complex changes so that it no longer inhibits the interaction between actin and myosin. This leads to tension producing cross bridges between actin and myosin, and ultimately muscle contraction [for reviews, see (*1*−*5*)].

One main cause of congestive heart failure is desensitization of the myocardium to Ca^{2+} as well as depressed cardiac contractility. Thus, the ability to sensitize cardiac muscle to Ca^{2+} and increase myocardial contractility would have promising therapeutic potential for the treatment of the disease. Great interest has been focused on the development of Ca^{2+}-sensitizing agents in the past decade. These drugs have been shown to sensitize the contractile proteins to Ca^{2+} without increase of cytosolic Ca^{2+} concentration [for reviews, see (*6*−*8*)]. The thiadiazinone derivative EMD 57033 is one of the Ca^{2+} sensitizers identified (*9*−*11*). It has been found to increase the Ca^{2+} sensitivity of both myofibrillar ATPase (*11*, *12*) and force development by skinned muscle fibers (*11*). However, the molecular mechanism underlining the Ca^{2+}-sensitizing effects of EMD 57033 is not well understood. It is possible that the compound interacts directly with troponin C and increases its affinity for Ca^{2+} (*13*). It is also possible that it exerts an effect on the interface of myosin−actin (*12*).

† Supported by the Medical Research Council of Canada, the Heart and Stroke Foundation of Canada, and the National Institutes of Health. L.S. is a Heart and Stroke Foundation of Canada Research Fellow.

* To whom correspondence should be addressed. E-mail: brian.sykes@ualberta.ca.

‡ University of Alberta.

§ E. Merck.

|| University of Texas Medical School.

[1] Abbreviations: TnC, troponin C; sTnC, skeletal muscle troponin C; cTnC, cardiac muscle troponin C; cTnC(A-Cys), C35S and C84S mutant of cTnC; TnI, troponin I; sTnI, skeletal muscle TnI; cTnI, cardiac muscle TnI; cIp, inhibitory synthetic peptide (128−147) of cardiac TnI; sIp, inhibitory synthetic peptide (96−115) of skeletal TnI; EMD, EMD 57033; NMR, nuclear magnetic resonance; HSQC, heteronuclear single-quantum coherence.

10.1021/bi000473i CCC: $19.00
Published on Web 06/30/2000

Cardiac troponin C is the Ca^{2+} binding component in the thin filament of cardiac muscle and an attractive target for potential Ca^{2+}-sensitizing compounds. Knowledge of the structure and surface topology of cTnC is critical for an understanding of how these compounds interact with cTnC. Until recently, most of the drug binding studies have relied on structural models of cardiac TnC derived from structures of skeletal TnC and calmodulin (*14*−*16*). As a result, an open conformation for the N-domain of cTnC was proposed, and the drugs were thought to bind to the hydrophobic surface. However, the recent NMR solution structures of intact Ca^{2+}-saturated cTnC (*17*) and the apo and Ca^{2+}-saturated N-domain of cTnC (*18*) reveal significant Ca^{2+}-induced structural differences between sTnC and cTnC with a closed N-domain for cTnC in the Ca^{2+}-saturated state. These structures have significant implications with respect to drug binding sites in cTnC. In this study, taking advantage of the availability of the high-resolution structure of cTnC and its completely assigned 2D {^{1}H,^{15}N}-HSQC NMR spectra, we monitored in detail the binding of EMD 57033 to cTnC and mapped its location on the structure of cTnC.

Another interesting issue is whether these Ca^{2+}-sensitizing compounds interfere with cTnI binding to cTnC. The interaction of cTnC and cTnI plays a central role in cardiac muscle contraction. Biochemical and biophysical studies have clarified how various regions of cTnI react with cTnC and participate in thin filament Ca^{2+} signaling [for a review, see (*3*)]. An antiparallel arrangement between cTnC and cTnI has been proposed (*19*), and an inhibitory region (residues 128−147) has been identified (*20*). A movement of the inhibitory region of cTnI from cTnC to actin−tropomyosin is believed to be the major switch between contraction and relaxation (*21*), and this switch is modulated by the interaction of the C-terminal region of cTnI and cTnC (*22*, *23*). Structural data on cardiac TnI include the structure of cTnI inhibitory peptide bound to cardiac TnC determined by Campbell et al. (*24*) and the structural information generated by using NMR and selective isotope labeling of Met residues in both cTnC and cTnI (*19*, *25*, *26*). The NMR solution structure of the complex of the N-domain of cTnC and the cTnI 147−163 region is the only high-resolution structure of the cTnC−cTnI binary complex available to date (*27*). To evaluate the possible competitive binding of EMD 57033 and cTnI on cTnC, we performed detailed titrations of cIp peptide binding to cTnC in the absence and presence of EMD 57033, respectively. EMD 57033 was also titrated into cTnC in the presence of cIp. The inhibitory peptide chosen is the critical functional region for cTnI interacting with cTnC (*28*). These titrations are monitored by 2D {^{1}H,^{15}N}-HSQC NMR spectroscopy, and the ligand-induced chemical shift changes are used to map the binding sites for EMD 57033 and cIp on cTnC. Together with the titration of EMD 57033 on cTnC, these studies reveal that both EMD 57033 and cIp bind to the C-domain of cTnC with 1:1 stoichiometry, but with noncompetitive binding sites, implying that EMD 57033 may not interfere with the interaction of cTnC and cIp. These findings suggest that EMD 57033 may exert its positive inotropic effect by not directly enhancing Ca^{2+} binding to the Ca^{2+} regulatory site of cTnC, but by binding to the structural domain of cTnC, modulating the interaction between cTnC and other thin filament proteins, and increasing the apparent Ca^{2+} sensitivity of the contractile system. This work provides new insight into the molecular mechanism underlining the Ca^{2+}-sensitizing effects of EMD 57033.

EXPERIMENTAL PROCEDURES

Sample Preparation. Recombinant chicken cardiac [^{15}N]-cTnC with the mutations C35S and C84S [denoted cTnC (A-Cys)] was used in this study. The expression and purification of cTnC (A-Cys) are as described previously (*17*). Since cTnC(A-Cys) is the only protein used throughout this work, (A-Cys) is omitted in this paper. Two portions of solid [^{15}N]-cTnC were dissolved separately into 500 μL of NMR buffer containing 100 mM KCl, 10 mM imidazole in 90% H_2O/10% D_2O. The sample concentrations were determined to be 0.70 and 0.56 mM, respectively, by amino acid analysis. To each sample was added 5 μL of 1 M $CaCl_2$ to ensure that the protein was Ca^{2+}-saturated, and the pH was adjusted by 1 M HCl to 6.7. The synthetic peptide cIp, acetyl-TQKIFDLRGKFKRPTLRRVR-amide, was prepared as described for the sIp peptide in Tripet et al. (*29*). The peptide was lyophilized twice to remove residual organic solvents. Solid cIp was dissolved in double distilled water to make two stock solutions, and the concentrations were 44 and 77 mM, respectively, as determined by amino acid analysis. E. Merck kindly provided EMD 57033. The chemical formula and properties of EMD 57033 are as described in Jonas et al. (*30*). The purity of the drug was checked by 1D ^{1}H NMR spectroscopy. Two stock solutions (53.3 and 106.5 mM, respectively, determined by UV absorption using a molar extinction coefficient $\epsilon_{1cm,320nm}$ = 20 000) of EMD 57033 in DMSO were prepared immediately before use, and the vials containing the solutions were wrapped in aluminum foil due to its sensitivity to light. Gilson Pipetman P (models P2 and P10) was used to deliver the drug or peptide solutions for all titrations.

(A) Titration of [^{15}N]-cTnC with EMD 57033. To an NMR tube containing a 500 μL sample of 0.70 mM [^{15}N]-cTnC were added aliquots of 1 μL of 53.3 mM EMD 57033 in DMSO for the first three titration points, and aliquots of 1 μL of 106.5 mM EMD 57033 in DMSO were added for the next three titration points. The sample was mixed thoroughly with each addition. After the sixth addition, a small amount of white precipitate was observed. This precipitate is likely unbound EMD 57033, which is insoluble in aqueous solution. The appearance also resembles that of solid EMD 57033 in aqueous solution. The total volume increase was 6 μL, and the change in protein concentration due to dilution was taken into account for data analyses. The change in pH from EMD 57033 addition was negligible. Both 1D ^{1}H and 2D {^{1}H, ^{15}N}-HSQC NMR spectra were acquired at every titration point. As a control experiment, a 2D {^{1}H,^{15}N}-HSQC NMR spectrum of [^{15}N]-cTnC in the presence of 6 μL of pure DMSO was acquired to test possible effects of DMSO on cTnC.

(B) Titration of [^{15}N]-cTnC with cIp. To an NMR tube containing a 500 μL sample of 0.56 mM [^{15}N]-cTnC was added 0.5 μL of 44 mM cIp for the first titration point, aliquots of 1 μL of 44 mM cIp were added for the following three titration points, aliquots of 1 μL of 77 mM cIp were added for the next four titration points, and aliquots of 2 μL of 77 mM cIp were added for the last two titration points. The sample was mixed thoroughly with each addition. The

total volume increase was 11.5 μL, and the change in protein concentration due to dilution was taken into account for data analyses. The change in pH from cIp addition was negligible. Both 1D ^{1}H and 2D {^{1}H, ^{15}N}-HSQC spectra were acquired at every titration point.

(*C) Titration of [^{15}N]-cTnC·cIp with EMD 57033*. Following titration B, the sample was filtered, and the appropriate amount of NMR buffer was added to generate a 500 μL NMR sample containing [^{15}N]-cTnC·cIp complex. The total cTnC concentration was 0.42 mM. Aliquots of 1 μL of 53.3 mM EMD 57033 were added for each point. The sample was mixed thoroughly with each addition. After the fifth addition, free EMD 57033 began to precipitate. The total volume increase was 5 μL, and the change in protein concentration due to dilution was taken into account for data analyses. The change in pH from EMD 57033 addition was negligible. Both 1D ^{1}H and 2D {^{1}H, ^{15}N}-HSQC NMR spectra were acquired at every titration point.

(D) Titration of [^{15}N]-cTnC·EMD 57033 with cIp. After titration A, the sample was filtered, and appropriate amount of NMR buffer was added to generate a 500 μL NMR sample of a 1:1 [^{15}N]-cTnC·EMD 57033 complex. The sample contains a total of 0.49 mM cTnC. One microliter of 44 mM cIp was added for the first titration point, aliquots of 1 μL of 77 mM cIp were added for the next four titration points, and aliquots of 2 μL of 77 mM cIp were added for the last two titration points. The sample was mixed thoroughly with each addition. Precipitation of free EMD 57033 was not observed during the titration. The total volume increase was 9 μL, and the change in protein concentration due to dilution was taken into account for data analyses. The change in pH from cIp addition was negligible. Both 1D ^{1}H and 2D {^{1}H, ^{15}N}-HSQC spectra were acquired at every titration point.

NMR Spectroscopy. All of the NMR spectra were obtained using a Unity INOVA 500 MHz spectrometer at 30 °C. The 2D {^{1}H, ^{15}N}-HSQC NMR spectra were acquired using the sensitivity-enhanced gradient pulse scheme developed by Lewis E. Kay and co-workers (*31*, *32*). The ^{1}H and ^{15}N sweep widths were 7000 and 1500 Hz, respectively. Spectral processing and analyses were accomplished with the programs NMRPipe (*33*) and PIPP (*34*), respectively. The chemical shift mapping technique was used to delineate the binding sites of EMD 57033 and cIp on the structure of cTnC. This approach has been demonstrated to be extremely useful for quickly identifying general sites of interaction between protein and ligand (*35*−*37*).

RESULTS

Figure 1A and 1B show the 2D {^{1}H,^{15}N}-HSQC NMR spectral changes for the titration of cTnC with EMD 57033 and cIp, respectively. Figure 2 shows the progressive shifts of 2D {^{1}H,^{15}N}-HSQC NMR spectra of residues Gly-140 and Ile-128 for the titration of cTnC with EMD 57033 (A), cTnC with cIp (B), cTnC·cIp with EMD 57033 (C), and cTnC·EMD 57033 with cIp (D), respectively. The binding curves for the four titrations are shown in Figure 3A−D. Figure 4A and 4B compare the respective EMD 57033 and cIp-induced chemical shift changes for cTnC along the cTnC sequence. Chemical shift mapping of the EMD 57033 and cIp binding sites on cTnC is shown in Figure 5B and 5C, respectively.

Effect of EMD 57033 on cTnC. The 2D {^{1}H,^{15}N}-HSQC NMR spectrum of cTnC(A-Cys) in the Ca^{2+}-saturated state is completely assigned (*17*) and used as a starting point to monitor EMD 57033-induced spectral changes. Figure 1A depicts the EMD 57033-induced backbone amide resonance changes in cTnC. The cross-peaks located outside of the most crowded area of the spectrum are labeled with the residue assignments. All the chemical shift changes fall into the fast exchange limit on the NMR time scale. The linear movement of the cross-peaks indicates that only two species exist in the interaction between the drug and the protein. The position of each cross-peak corresponds to the weighted average of the bound and free chemical shifts of cTnC. This phenomenon was also observed in our earlier studies on Ca^{2+} and cTnI 147−163 binding to cNTnC (*27*). Multiple binding of EMD 57033 to protein would result in cross-peak-shifting in a nonlinear fashion in the 2D {^{1}H,^{15}N}-HSQC NMR spectrum, as observed in the case of TFP binding to cTnC (*38*). It is important to note that DMSO has no effect on the 2D {^{1}H,^{15}N}-HSQC NMR spectrum of cTnC (data not shown).

Resonances of residues that undergo backbone amide ^{1}H or ^{15}N chemical shift changes during titration can be followed to monitor EMD 57033 binding to the protein. Plots of EMD 57033-induced chemical shift changes of individual amides of cTnC as a function of the $[EMD]_{total}/[cTnC]_{total}$ ratio gave similar curves, and the average curve for all monitored amides is shown in Figure 3A. The normalized average chemical shift data as a function of $[EMD]_{total}/[cTnC]_{total}$ for those amides were fit to the following equation [see Li et al. (*27*) and references cited therein]:

$$\text{cTnC} + \text{EMD} \rightleftharpoons \text{cTnC·EMD} \qquad (1)$$

and yielded a macroscopic dissociation constant (K_D) of 8.0 ± 1.8 μM, indicating a tight and stable 1:1 cTnC·EMD 57033 complex.

Inspection of Figure 1A indicates that cross-peaks corresponding to residues located in the N-domain of cTnC are not shifted upon the addition of EMD 57033. Thr-13, Gly-42, Glu-55, Glu-66, Gly-70, and Lys-90 are typical examples. On the other hand, residues located in the C-domain, for example, Leu-117, Ile-128, Gly-140, Lys-142, and Glu-155, undergo large EMD 57033-induced shifts. The absolute chemical shift changes in both ^{1}H and ^{15}N dimensions were normalized, respectively, such that $\Delta\delta_{ppm} = 1$ for each residue represents the average change for all residues. The normalized values for ^{1}H and ^{15}N were averaged and plotted against the protein sequence (Figure 4A). This plot shows that most of the residues located in the C-domain are more or less affected by EMD 57033 binding, but 17 residues (as labeled in Figure 4A) undergo significant ($\Delta\delta_{ppm} \geq 1.5$) chemical shift perturbations. Mapping of these residues on the structure of cTnC (Figure 5B) reveals clearly a contiguous binding surface for EMD 57033.

Effect of cIp on cTnC. Similar to monitoring EMD 57033 binding to cTnC, the 2D {^{1}H,^{15}N}-HSQC NMR spectrum of cTnC in the Ca^{2+}-saturated state is used as a starting point to monitor cIp-induced spectral changes. Figure 1B depicts cIp-induced backbone amide resonance shifts in cTnC. The cross-peaks located outside of the most crowded area of the spectrum are labeled with the residue assignments. All of

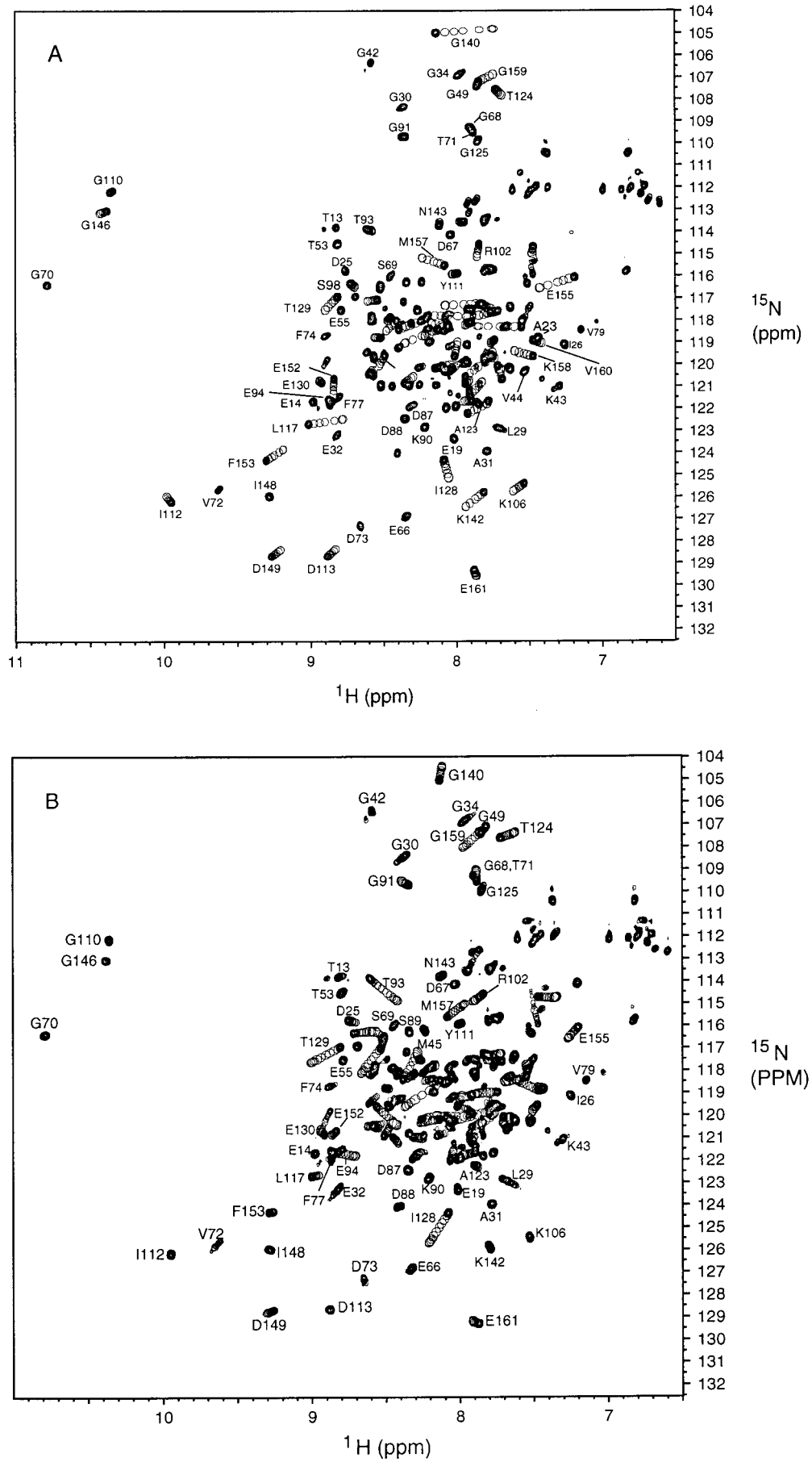

FIGURE 1: Titration of (A) cTnC with EMD 57033 and (B) cTnC with cIp. 2D {^{1}H, ^{15}N}-HSQC NMR spectra from the backbone amide regions of cTnC at various EMD 57033 or cIp additions are superimposed, showing the progressive shift of peaks with increasing EMD 57033 or cIp concentrations. Conditions are as described under Experimental Procedures.

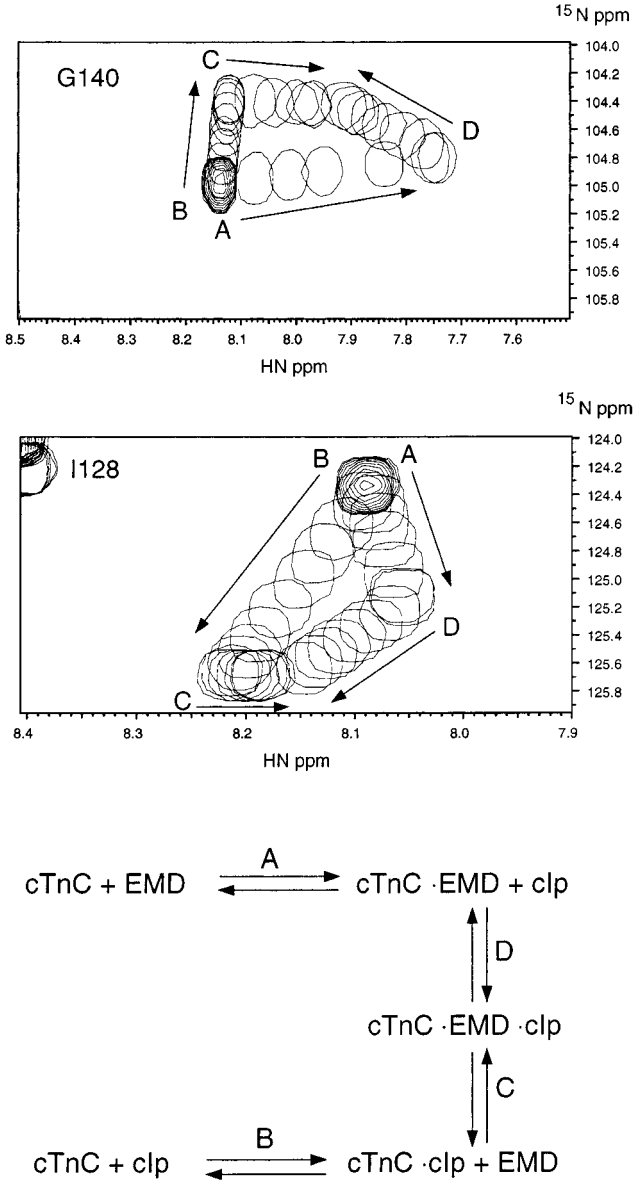

FIGURE 2: Titration of (A) cTnC with EMD 57033, (B) cTnC with cIp, (C) cTnC·cIp with EMD 57033, and (D) cTnC·EMD 57033 with cIp. 2D {^{1}H, ^{15}N}-HSQC NMR spectra for residues Gly-140 and Ile-128 of cTnC at various EMD 57033 or cIp additions are superimposed, showing the progressive shift of peaks with increasing EMD 57033 or cIp concentrations. The corresponding equilibria for titrations A−D are also shown. Conditions are as described under Experimental Procedures.

the chemical shift changes fall into the fast exchange limit on the NMR time scale. The linear movement of the cross-peaks indicates the interaction between the peptide and the protein occurs with a 1:1 stoichiometry, as observed in the case of EMD 57033.

Plots of cIp-induced chemical shift changes of individual amides of cTnC as a function of the $[cIp]_{total}/[cTnC]_{total}$ ratio gave similar curves, and the average curve for all monitored amides is shown in Figure 3B. The normalized average chemical shift data as a function of $[cIp]_{total}/[cTnC]_{total}$ for all amides were fit to the equation:

$$cTnC + cIp \rightleftharpoons cTnC{\cdot}cIp \qquad (2)$$

and yielded a macroscopic dissociation constant (K_D) of 78.2 ± 10.3 μM. This affinity is approximately 10 times weaker than EMD 57033 binding to cTnC.

Comparing Figures 1A and 1B reveals both similarities and differences. They are similar in terms of C-domain residues; for example, Ile-128, Gly-140, and Glu-155, experience large cIp-induced shifts, while residues located in the N-domain undergo small or no cIp-induced shifts. However, the differences are more prevalent. Residues that shift in both Figures 1A and 1B, such as Ile-128, Gly-140, and Gly-159, move in different directions. Residues such as Asp-113, Leu-117, Lys-142, and Phe-153 undergo large EMD 57033-induced chemical shift changes (Figure 1A), but small cIp-induced shifts (Figure 1B). Interestingly, residues located in the central linker between the N- and C-domains of cTnC undergo large cIp-induced chemical shift perturbation, but negligible EMD 57033-induced changes. Thr-93 is a typical example. It is worth noting that some residues from the N-domain (for example, Asp-25, Gly-30, and Gly-34) also move slightly in response to cIp binding but not to EMD 57033 binding. This is probably due to the effect of the peptide on the central linker.

Careful tracing of chemical shift changes for every residue from the beginning to the end of the titration followed by normalization in both ^{1}H and ^{15}N dimensions allowed the assessment of cIp binding on cTnC sequence. The normalized values for ^{1}H and ^{15}N were averaged and plotted against the protein sequence (Figure 4B). The plot shows that residues encompassing Ca^{2+} binding site III are obviously more perturbed than those located in EF hand helix G-loop IV-helix H. As compared to Figure 4A, the region from Lys-90 to Lys-97 is significantly affected by peptide (Figure 4B) but not at all by the drug (Figure 4A). The 14 residues that undergo significant ($\Delta\delta_{ppm} \geq 1.5$) chemical shift changes are labeled in Figure 4B and are mapped to the surface of cTnC (Figure 5C). Discrete patches of color on the surface of cTnC represent the binding site for cIp. Figure 5 shows different binding modes for the drug and the peptide, suggesting that they may not compete with each other for cTnC.

Effect of EMD 57033 on cTnC·cIp. When EMD 57033 is titrated into the cTnC·cIp complex, additional chemical shift changes are induced, and the changes do not reverse those induced by cIp on cTnC, indicating the drug may not disrupt the cTnC·cIp complex. In fact, the 2D{^{1}H,^{15}N}-HSQC NMR spectrum of cTnC·cIp·EMD does not superimpose with those of cTnC, cTnC·EMD, or cTnC·cIp, indicating the formation of a ternary complex. Using Gly-140 and Ile-128 as examples, Figure 2 demonstrates the EMD 57033-induced peak shifts in the absence (arrow A) and presence of cIp (arrow C). The normalized average chemical shift data as a function of $[EMD]_{total}/[cTnC]_{total}$ for monitored amides were fit to the equation:

$$cTnC{\cdot}EMD + cIp \rightleftharpoons cTnC{\cdot}EMD{\cdot}cIp \qquad (3)$$

and yielded a macroscopic dissociation constant (K_D) of 7.4 ± 4.8 μM (Figure 3C). This affinity, within experimental error, agrees with that for EMD 57033 binding to cTnC, suggesting that the drug interacts the same way with cTnC regardless of the presence of cIp.

Effect of cIp on cTnC·EMD. When cIp is titrated into the cTnC·EMD complex, additional chemical shift changes are

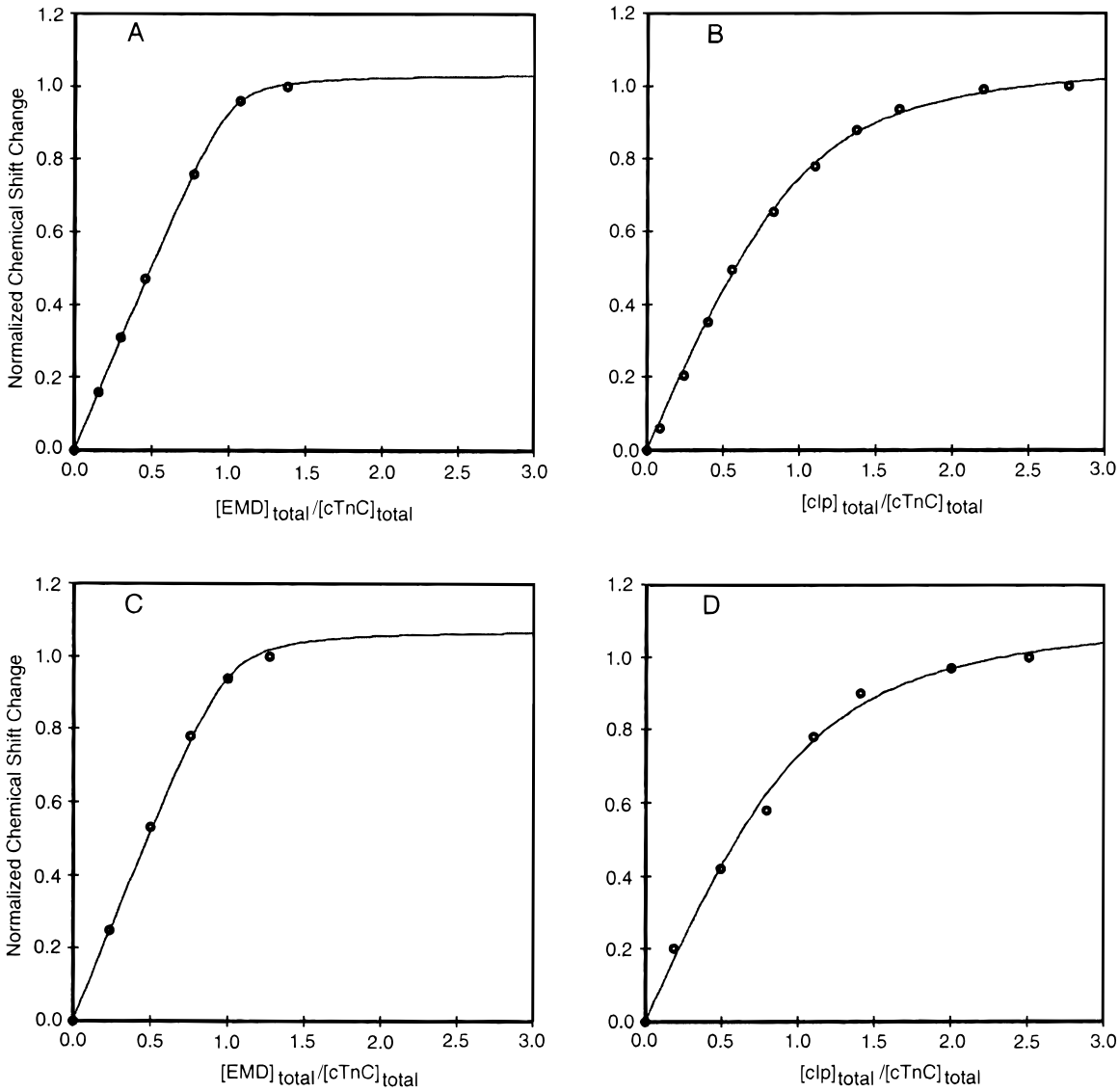

FIGURE 3: Titration of (A) cTnC with EMD 57033, (B) cTnC with cIp, (C) cTnC·cIp with EMD 57033, and (D) cTnC·EMD 57033 with cIp. The curve represents the average of residues affected by ligand binding as shown in Figure 1A, Figure 1B, and Figure 2, respectively. The curve is normalized according to $(\delta_{obs} - \delta_{initial}) /(\delta_{final} - \delta_{initial})$. A solid line represents the best fit to the data. Conditions are as described under Experimental Procedures.

induced, and the changes do not reverse those induced by EMD 57033 on cTnC, indicating the peptide is not displacing the bound drug. In fact, the 2D{^{1}H,^{15}N}-HSQC NMR spectrum of cTnC·EMD·cIp does not superimpose with those of cTnC, cTnC·EMD, or cTnC·cIp, indicating the formation of a ternary complex. Using Gly-140 and Ile-128 as examples, Figure 2 shows the cIp-induced peak shifts on cTnC (arrow B) and on the cTnC·EMD complex (arrow D). It is interesting to notice that arrows C and D point to the same end position. This indicates that the ternary complex cTnC·EMD·cIp formed from this titration is the same as the cTnC·cIp·EMD complex resulting from the previous titration. The normalized average chemical shift data as a function of $[cIp]_{total}/[cTnC]_{total}$ for all monitored amides were fit to the equation:

$$cTnC{\cdot}EMD + cIp \rightleftharpoons cTnC{\cdot}EMD{\cdot}cIp \qquad (4)$$

and yielded a macroscopic dissociation constant (K_D) of 99.2 ± 30.0 μM (Figure 3D). This affinity, within experimental error, agrees with the K_D for cIp binding to cTnC, suggesting the bound drug does not interfere with the interaction between cTnC and the inhibitory peptide.

DISCUSSION

In this paper, we have addressed two important issues regarding (1) whether the Ca^{2+} sensitizer EMD 57033 interacts directly with cardiac TnC and increases its affinity for Ca^{2+}, and (2) whether EMD 57033 competes with cardiac TnI (cTnI) for cTnC and interferes with the inhibitory function. To achieve the goal, we have used 2D {^{1}H,^{15}N}-HSQC NMR spectroscopy to monitor in detail the binding of EMD 57033 to Ca^{2+}-saturated cTnC in the absence and presence of cIp, respectively, and that of cIp in the absence and presence of EMD 57033, respectively. Since 2D {^{1}H,^{15}N}-HSQC NMR spectroscopy can report information pertaining to individual atoms throughout the protein sequence, we are able to detect the effect of EMD 57033 or cIp binding on all backbone amides of cTnC under various conditions. These studies allow the identification of binding sites of EMD 57033 and cIp on the structure of cTnC.

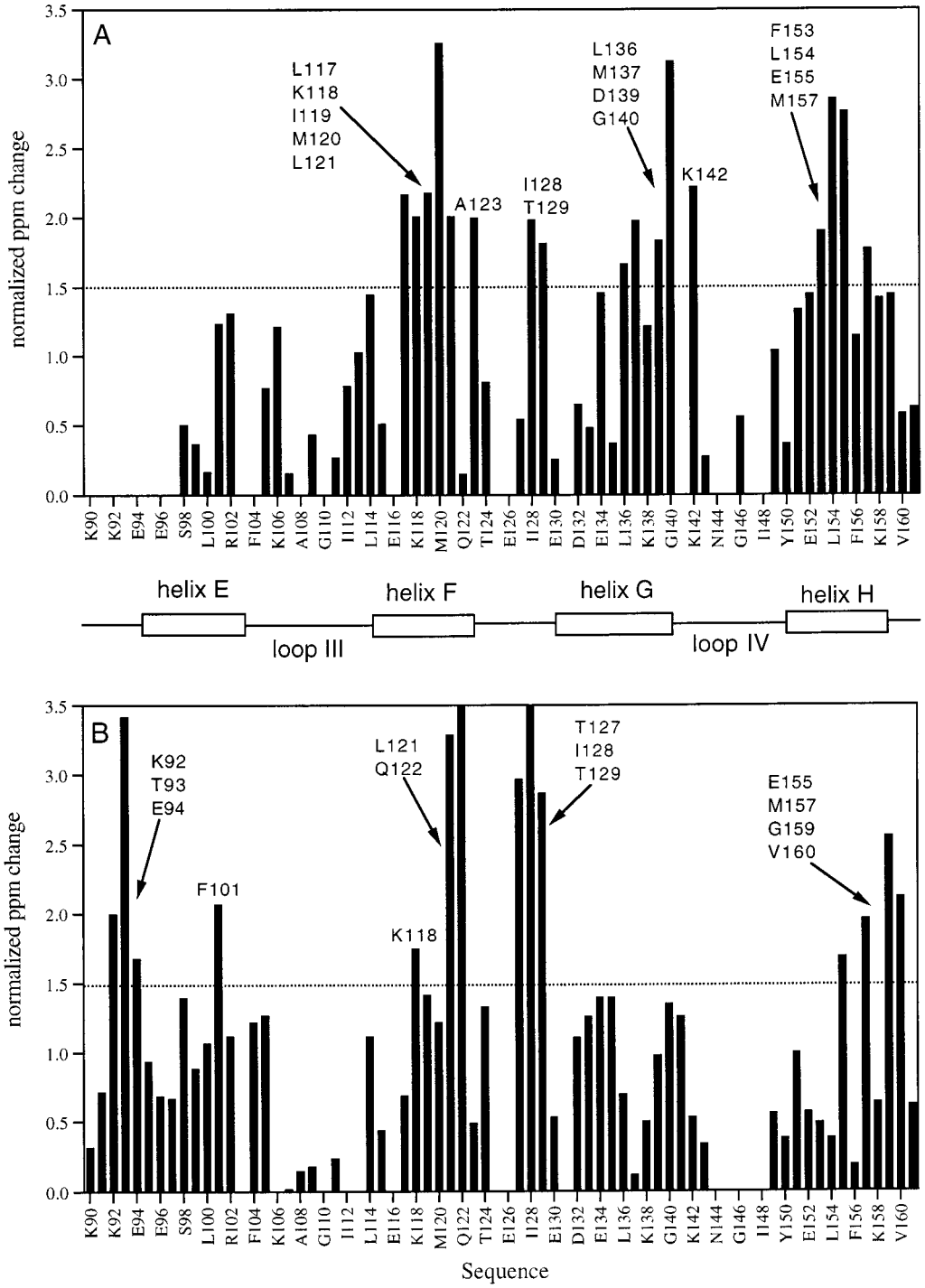

FIGURE 4: Comparison of EMD 57033 (A) and cIp (B) induced chemical shift changes for cTnC. The chemical shift changes for each residue were calculated by averaging the normalized chemical shift change of the backbone ^{1}H and ^{15}N chemical shifts. For a particular nucleus, the normalized chemical shift change of a residue is obtained by dividing the observed shift change by the average shift change for all residues. Thus, $\Delta\delta_{ppm} = 1$ indicates that the chemical shift change for a given residue is equal to the average change for all residues.

Previously, we have used the same method to characterize Ca^{2+} binding to skeletal and cardiac TnC (*39*, *40*) and to map the binding site for several skeletal and cardiac TnI peptides to the structure of skeletal TnC and cardiac TnC (*27*, *41*, *42*). Very recently, we investigated the competitive binding of the inhibitory (sTnI 96−115) and the N-terminal (Rp40) regions of skeletal TnI to the C-domain of skeletal TnC (*43*). Here we demonstrate again the power of 2D $\{^{1}H,^{15}N\}$-HSQC NMR spectroscopy in determining the stoichiometry and affinity of target binding to cTnC and in identifying the binding sites of targets on the structure of cTnC.

Two previous studies have shown that EMD 57033 interacts with the C-domain of cTnC (*44*, *45*). Using fluorescence spectroscopy, Pan and Johnson (*44*) have shown that EMD 57033 selectively binds to the Ca^{2+}-saturated C-domain of cTnC with a K_D of approximately 40 μM, but does not increase the Ca^{2+} affinity of regulatory site II. Kleerekoper and Putkey have shown that EMD 57033 induces chemical shift changes of Met methyl groups in the

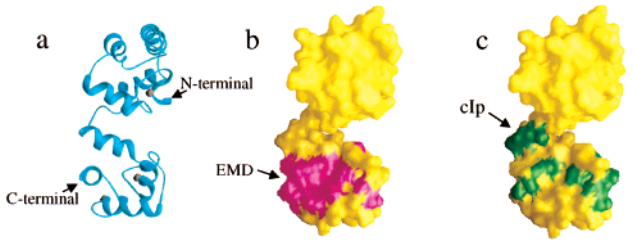

FIGURE 5: Ribbon representation of the NMR structure of cTnC (PDB code 1AJ4) (a) and molecular surfaces of cTnC in complex with EMD 57033 (b) and cIp (c). A view of the figure after a 180° rotation along the *y* axis does not show an interaction by either EMD 57033 or cIp with the other side of the protein. The EMD 57033 (b) and cIp (c) binding sites are identified by using chemical shift mapping and colored in purple and green, respectively. The figure was created by GRASP (*53*).

C-domain, but not in the N-domain (*45*). However, the exact binding site was not identified. Pan and Johnson (*44*) suggested that both Tyr-111 and Tyr-150 be in close proximity to the bound drug since the tyrosine fluorescence of cTnC was substantially quenched by EMD 57033. Kleerekoper and Putkey reported significant drug-induced chemical shift changes for Met-120 and Met-157 (*45*). Our results agree with those studies that the drug binds 1:1 to the C-domain of cTnC with no effect on the N-domain. In addition, we identified 14 residues (labeled in Figure 4A) which undergo significant drug-induced chemical shift changes and together they form a contiguous patch on the surface of the C-domain, the binding site for EMD 57033. The identified residues include Met-120 and Met-157, but not Tyr-111 and Tyr-150. It is interesting to note that the EMD 57033 binding site is not completely located in the exposed hydrophobic pocket on the C-domain (Figure 5B), but rather to the left side of the pocket. The hydrophobic patch located in the Ca^{2+}-saturated C-domain of cTnC has long been proposed as the cTnI binding site, and the residues located outside or on the opposite surface may interact with TnT, tropomyosin, or other contractile proteins (*46*). This observation implies that the drug may achieve its effect by modulating the interaction of cTnC with other thin filament proteins in addition to cTnI, enhancing the apparent Ca^{2+} binding affinity of the system, and partially restoring cardiac contractility.

The determined EMD 57033 binding affinity for cTnC is ~8 μM. This is approximately 5 times lower than the value reported by tyrosine fluorescence titration measurement (*44*). This discrepancy probably results from different experimental conditions between fluorescence and NMR methods. The affinity of the cTnC−EMD 57033 complex at the level of 40 μM is much higher than the concentration of EMD 57033 used in functional studies, while an 8 μM affinity is closer to the drug concentration. EMD 57033 is known to exert detectable positive inotropic effects on isolated cardiac myocytes at concentrations as low as 1 μM (*12*), and in skinned cardiac muscle fibers, less than 10 μM EMD 57033 induced significant Ca^{2+} sensitivity of force development (*11*). However, cTnC does not act alone, and the contractile proteins work in a highly organized and cooperative manner in muscle contraction [for a review, see (*2*)]. It is possible that cTnC in myofilaments may have a higher affinity for EMD 57033 than it does when cTnC is isolated in solution.

The noncompetitive binding sites based on chemical shift mapping of EMD 57033 and cIp on cTnC suggest that cTnI does not inhibit the binding of EMD 57033 to cTnC, and vice versa. Although cIp constitutes a small segment of cTnI, it encompasses the important inhibitory region of cTnI, and functional studies have shown that a major switch between muscle contraction/relaxation involves a movement of this region of TnI from TnC to actin−tropomyosin (*21*). In contrast to the contiguous binding surface for EMD 57033, the binding site for cIp consists of discrete patches on cTnC (see Figure 5). Although structural data are not available for cIp peptide in isolation or in complex with cTnC, a number of earlier studies have concluded that cIp interacts primarily with the C-domain of cTnC (*25*, *47*−*49*). NMR studies on the inhibitory region of skeletal TnI 96−115 have shown that this peptide binds sTnC in an extended form (*50*). Recently, we have mapped the binding site for sTnI 96−115 to the C-domain of sTnC (*43*). The epitope of cIp on cTnC is strikingly similar to that of sTnI 96−115 on sCTnC. This is not surprising considering the 85% sequence homology between cTnI 128−147 and sTnI 96−115. The association constant of 78 μM of cIp for cTnC is comparable to that of sIp for sCTnC (K_D = 47 μM). Together, these results suggest that cTnC-bound cIp adopts an extended conformation that stretches across the hydrophobic surface of the C-domain.

The results presented here show clearly that EMD 57033 does not compete with cIp for cTnC and interfere with the inhibitory function. A pertinent question is whether this is also the case with intact cTnI. Two regions of cTnI, cTnI 33−80 and cTnI 128−147, are implicated in binding to the C-domain of cTnC (*29*). A recent NMR study has shown that cTnI 33−80 binds to the hydrophobic pocket of C-domain (*51*). The X-ray structure of sTnC in complex with sTnI 1−47 shows that the corresponding region of sTnI 3−33 forms a long α-helix and fits into the hydrophobic groove of the C-domain (*52*). We have shown that sTnI 1−40 binds strongly to sCTnC with a K_D of ~2 μM and can displace sTnI 96−115 completely (*43*). In addition, it is likely that in order for the inhibitory region to bind to the C-domain of TnC to release inhibition, other factors, such as interactions between the N-domain of TnC with the C-domain of TnI or the C-domain of TnT, are required (*29*). It is interesting that the binding epitope of EMD 57033 on cTnC overlaps partially with that of sTnI 1−40 on sTnC [see Figure 5 in this paper and Figure 6 in (*43*)]. Thus, it is possible that the drug blocks the interaction between the N-terminal region of TnI and the C-terminal region of TnC and, consequently, enhances the binding of the inhibitory region of TnI to TnC. From the data presented here, it is likely that the drug plays a similar role as the C-domain of cTnI does in the interaction between the N-terminal domain of cTnC and the C-terminal domain of cTnI. Since this interaction is dependent on Ca^{2+} binding to the N-domain of cTnC, the apparent Ca^{2+} sensitivity of the contractile system can be modulated by EMD 57033.

CONCLUSIONS

This study was undertaken to investigate the interaction of cTnC with its targets: Ca^{2+} sensitizer EMD 57033 and cTnI 128−147 inhibitory peptide. Detailed titrations reveal that both targets bind to cTnC in 1:1 ratios and form stable

complexes ($K_D = 8\ \mu M$ for EMD 57033 and $K_D = 78\ \mu M$ for cIp). Neither is EMD 57033 binding affected by cIp nor does the drug affect cIp binding. In the end, a stable ternary cTnC·EMD·cIp complex is formed. Using the NMR solution structure of cTnC as a framework (*17*), the target binding sites are identified by using chemical shift mapping. The study demonstrates that EMD 57033 and cIp do not share common epitopes on cTnC although both interact with the C-terminal domain of cTnC, indicating that the drug does not interfere with the interaction of cTnC and the inhibitory region of cTnI. This study has profound implications in understanding the mechanism underlining Ca^{2+}-sensitizing effects of EMD 57033 in cardiac muscle.

ACKNOWLEDGMENT

We are indebted to Mr. Robert Boyko for his assistance with the curve fitting program, and to Drs. Ryan McKay and Brian Tripet for insightful discussions.

REFERENCES

1. Farah, C. S., and Reinach, F. C. (1995) *FASEB J. 9*, 755−767.
2. Tobacman, L. S. (1996) *Annu. Rev. Physiol. 58*, 447−481.
3. Solaro, R. J., and Rarick, H. M. (1998) *Circ. Res. 83*, 471−480.
4. Perry, S. V. (1999) *Mol. Cell. Biochem. 190*, 9−32.
5. Filatov, V. L., Katrukha, A. G., Bulargina, T. V., and Gusev, N. B. (1999) *Biochemistry (Moscow) 64*, 969−985.
6. Endoh, M. (1995) *Gen. Pharmacol. 26*, 1−31.
7. Varro, A., and Papp, J. G. (1995) *J. Cardiovasc. Pharmacol. 26*, S32−44.
8. Nielsen-Kudsk, J. E., and Aldershvile, J. (1995) *J. Cardiovasc. Pharmacol. 26*, S77−84.
9. Ventura, C., Miller, R., Wolf, H. P., Beier, N., Jonas, R., Klockow, M., Lues, I., Hano, O., Spurgeon, H. A., Lakatta, E. G., and et al. (1992) *Circ. Res. 70*, 1081−1090.
10. Gross, T., Lues, I., and Daut, J. (1993) *J. Mol. Cell Cardiol. 25*, 239−244.
11. Lues, I., Beier, N., Jonas, R., Klockow, M., and Haeusler, G. (1993) *J Cardiovasc. Pharmacol. 21*, 883−892.
12. Solaro, R. J., Gambassi, G., Warshaw, D. M., Keller, M. R., Spurgeon, H. A., Beier, N., and Lakatta, E. G. (1993) *Circ. Res. 73*, 981−990.
13. Lee, J. A., and Allen, D. G. (1990) *Br. Med. J. 300*, 551−552.
14. MacLachlan, L. K., Reid, D. G., Mitchell, R. C., Salter, C. J., and Smith, S. J. (1990) *J. Biol. Chem. 265*, 9764−9770.
15. Ovaska, M., and Taskinen, J. (1991) *Proteins: Struct., Funct., Genet. 11*, 79−94.
16. Pollesello, P., Ovaska, M., Kaivola, J., Tilgmann, C., Lundstrom, K., Kalkkinen, N., Ulmanen, I., Nissinen, E., and Taskinen, J. (1994) *J. Biol. Chem. 269*, 28584−28590.
17. Sia, S. K., Li, M. X., Spyracopoulos, L., Gagné, S. M., Liu, W., Putkey, J. A., and Sykes, B. D. (1997) *J. Biol. Chem. 272*, 18216−18221.
18. Spyracopoulos, L., Li, M. X., Sia, S. K., Gagné, S. M., Chandra, M., Solaro, R. J., and Sykes, B. D. (1997) *Biochemistry 36*, 12138−12146.
19. Krudy, G. A., Kleerekoper, Q., Guo, X., Howarth, J. W., Solaro, R. J., and Rosevear, P. R. (1994) *J. Biol. Chem. 269*, 23731−23735.
20. Talbot, J. A., and Hodges, R. S. (1981) *J. Biol. Chem. 256*, 2798−2802.
21. Van Eyk, J. E., and Hodges, R. S. (1988) *J. Biol. Chem. 263*, 1726−1732.
22. Rarick, H. M., Tu, X. H., Solaro, R. J., and Martin, A. F. (1997) *J. Biol. Chem. 272*, 26887−26892.
23. Ramos, C. H. (1999) *J. Biol. Chem. 274*, 18189−18195.
24. Campbell, A. P., Van Eyk, J. E., Hodges, R. S., and Sykes, B. D. (1992) *Biochim. Biophys. Acta 1160*, 35−54.
25. Howarth, J. W., Krudy, G. A., Lin, X., Putkey, J. A., and Rosevear, P. R. (1995) *Protein Sci. 4*, 671−680.
26. Kleerekoper, Q., Howarth, J. W., Guo, X., Solaro, R. J., and Rosevear, P. R. (1995) *Biochemistry 34*, 13343−13352.
27. Li, M. X., Spyracopoulos, L., and Sykes, B. D. (1999) *Biochemistry 38*, 8289−8298.
28. Van Eyk, J. E., Kay, C. M., and Hodges, R. S. (1991) *Biochemistry 30*, 9974−9981.
29. Tripet, B. P., Van Eyk, J. E., and Hodges, R. S. (1997) *J. Mol. Biol. 271*, 728−750.
30. Jonas, R., Klockow, M., and Lues, I. (1992) *Bioorg. Med. Chem. Lett. 2*, 589−592.
31. Kay, L. E., Keifer, P., and Saarinen, T. (1992) *J. Am. Chem. Soc. 114*, 10663−10665.
32. Zhang, O., Kay, L. E., Olivier, J. P., and Forman-Kay, J. D. (1994) *J. Biomol. NMR 4*, 845−858.
33. Delaglio, F., Grzesiek, S., Vuister, G. W., Zhu, G., Pfeifer, J., and Bax, A. (1995) *J. Biomol. NMR 6*, 277−293.
34. Garrett, D. S., Powers, R., Gronenborn, A. M., and Clore, G. M. (1991) *J. Magn. Reson. 95*, 214−220.
35. Shuker, S. B., Hajduk, P. J., Meadows, R. P., and Fesik, S. W. (1996) *Science 274*, 1531−1534.
36. Sun, C., Cai, M., Gunasekera, A. H., Meadows, R. P., Wang, H., Chen, J., Zhang, H., Wu, W., Xu, N., Ng, S. C., and Fesik, S. W. (1999) *Nature 401*, 818−822.
37. Medek, A., Hajduk, P. J., Mack, J., and Fesik, S. W. (2000) *J. Am. Chem. Soc. 122*, 1241−1242.
38. Kleerekoper, Q., Liu, W., Choi, D., and Putkey, J. A. (1998) *J. Biol. Chem. 273*, 8153−8160.
39. Li, M. X., Gagné, S. M., Tsuda, S., Kay, C. M., Smillie, L. B., and Sykes, B. D. (1995) *Biochemistry 34*, 8330−8340.
40. Li, M. X., Gagné, S. M., Spyracopoulos, L., Kloks, C. P. A. M., Audette, G., Chandra, M., Solaro, R. J., Smillie, L. B., and Sykes, B. D. (1997) *Biochemistry 36*, 12519−12525.
41. McKay, R. T., Tripet, B. P., Hodges, R. S., and Sykes, B. D. (1997) *J. Biol. Chem. 272*, 28494−28500.
42. McKay, R. T., Pearlstone, J. R., Corson, D. C., Gagne, S. M., Smillie, L. B., and Sykes, B. D. (1998) *Biochemistry 37*, 12419−12430.
43. Mercier, P., Li, M. X., and Sykes, B. D. (1999) *Biochemistry 38*, 1−2.
44. Pan, B.-S., and Johnson, J., R. G. (1996) *J. Biol. Chem. 271*, 817−823.
45. Kleerekoper, Q., and Putkey, J. A. (1999) *J. Biol. Chem. 274*, 23932−23939.
46. Herzberg, O., Moult, J., and James, M. N. G. (1986) *J. Biol. Chem. 261*, 2638−2644.
47. Lan, J., Albaugh, S., and Steiner, R. F. (1989) *Biochemistry 28*, 7380−7385.
48. Swenson, C. A., and Fredricksen, R. S. (1992) *Biochemistry 31*, 3420−3429.
49. Ngai, S.-M., Sönnichsen, F. D., and Hodges, R. S. (1994) *J. Biol. Chem. 269*, 2165−2172.
50. Hernandez, G., Blumenthal, D. K., Kennedy, M. A., Unkefer, C. J., and Trewhella, J. (1999) *Biochemistry 38*, 6911−6917.
51. Gasmi-Seabrook, G. M., Howarth, J. W., Finley, N., Abusamhadneh, E., Gaponenko, V., Brito, R. M., Solaro, R. J., and Rosevear, P. R. (1999) *Biochemistry 38*, 8313−8322.
52. Vassylyev, D. G., Takeda, S., Wakatsuki, S., Maeda, K., and Maeda, Y. (1998) *Proc. Natl. Acad. Sci. U.S.A 95*, 4847−4852.
53. Nicholls, A. (1992) *GRASP: graphical representation and analysis of surface properties*, Columbia University, New York.

BI000473I